

Decoupling of unpolluted temperate forests from rock nutrient sources revealed by natural $^{87}\text{Sr}/^{86}\text{Sr}$ and ^{84}Sr tracer addition

Martin J. Kennedy*[†], Lars O. Hedin[‡], and Louis A. Derry[§]

*Department of Earth Science, University of California, Riverside, CA 92521; [†]Department of Ecology and Evolutionary Biology and Princeton Environmental Institute, Princeton University, Princeton, NJ 08544-1003; and [§]Department of Earth and Atmospheric Sciences, Cornell University, Ithaca, NY 14853

Edited by Peter Vitousek, Stanford University, Stanford, CA, and approved May 30, 2002 (received for review January 25, 2002)

An experimental tracer addition of ^{84}Sr to an unpolluted temperate forest site in southern Chile, as well as the natural variation of $^{87}\text{Sr}/^{86}\text{Sr}$ within plants and soils, indicates that mechanisms in shallow soil organic horizons are of key importance for retaining and recycling atmospheric cation inputs at scales of decades or less. The dominant tree species *Nothofagus nitida* feeds nearly exclusively (>90%) on cations of atmospheric origin, despite strong variations in tree size and location in the forest landscape. Our results illustrate that (i) unpolluted temperate forests can become nutritionally decoupled from deeper weathering processes, virtually functioning as atmospherically fed ecosystems, and (ii) base cation turnover times are considerably more rapid than previously recognized in the plant available pool of soil. These results challenge the prevalent paradigm that plants largely feed on rock-derived cations and have important implications for understanding sensitivity of forests to air pollution.

Reports of diminished base cations (Ca^{2+} , Mg^{2+} , K^{+} , and Na^{+}) in sensitive soils have raised concerns over whether acid rain (1–6), reductions in atmospheric base cations (7–8), and forest cutting (9) are degrading forest ecosystems in temperate regions of Europe and North America (10, 11). Studies thus far have focused on regions where biogeochemical cycles are already strongly disturbed by human activities (1–14). To understand natural biogeochemical cycles, we consider here temperate rainforests in southern Chile that have not been exposed to acid rain or other significant anthropogenic influences (15).

Forests of the Cordillera Piuchué Ecosystem Study (CPES; 42°22' S, 74°03' W) are in contact with among the least polluted atmospheres in the world (15, 16). Precipitation chemistry is nearly exclusively dominated by dilute sea-salt aerosols delivered by persistent westerly winds from the southern Pacific Ocean (15). The broad-leaved CPES rainforests are diverse in tree species composition, have high basal areas (approximately 50–90 m^2/ha) and canopy heights of ≈ 30 m, receive 500–700 cm annual precipitation [of which approximately 17–28% falls in summer (December–March $n = 3$ yr)], and are underlain by thin unglaciated soils (<50–60 cm of mineral soil on top of saprolite) on Precambrian mica schist bedrock (15, 17). Soils are acidic and contain a thick organic horizon (≈ 0 –25 cm) with high fine root biomass.

To determine the source and cycling of plant-available base cation nutrients in CPES soils and plants, we conducted Sr isotopic studies. Although Sr^{2+} is not a plant nutrient or important weathering product, it closely tracks Ca^{2+} chemistry because of its similar charge and ionic radius (Fig. 1). It serves as a useful proxy for Ca^{2+} (and to a lesser degree other base cations) for tracing weathering processes because it has several isotopes that can be used to determine the rock weathering versus atmospheric contributions to base cation pools within soil-plant systems (4, 12–14, 18, 19). We adopted two independent strategies in our Sr isotopic study. In the first, we characterized the natural isotopic abundance of $^{87}\text{Sr}/^{86}\text{Sr}$ within plants, soils, rocks, and ground water to determine the long-term, steady-state

sources of cations to the system. Our second strategy focused on the dynamic behavior of the system. We simulated a rainfall event with “precipitation” labeled with stable ^{84}Sr . We then monitored the movement of this tracer through the soil and plants over 715 days to determine the kinetics of atmospherically derived exchangeable bases.

Methods

For natural Sr^{2+} abundance studies we collected plant materials within ≈ 5 ha forested area, including a 700-m transect from upland to lowland habitats. Tree cores and leaves were dried, ashed, and digested in ultra-pure, double-distilled nitric and perchloric acid. Bedrock and saprolite samples were collected from surface outcrops in close proximity to soil profiles, and water samples were collected in adjacent streams as per ref. 15.

To examine mechanisms and temporal scales over which CPES forests retain atmospherically derived cations, we selected an 18.5 m^2 study plot that was located on a ridge crest, not subject to down-slope hydrologic flow. We simulated a 10-mm rain event by spraying this forest plot with a dilute solution of isotopically enriched $^{84}\text{SrCO}_3$ (56 μg Sr/liter; $^{84}\text{Sr}/^{86}\text{Sr} = 18.020$). This solution was produced by dissolving 19 mg of $^{84}\text{SrCO}_3$ in 200 liters of stream water and applied to the study area with a sprayer. The stable ^{84}Sr isotope is a particularly sensitive tracer for Sr^{2+} since the $^{84}\text{Sr}/^{86}\text{Sr}$ ratio is invariant in nature (0.0565) and ^{84}Sr comprises only 0.56% of total Sr. This tracer addition could have only a minimal effect on chemical behavior of the system as it comprised <1% of the total Sr pool, while altering the $^{84}\text{Sr}/^{86}\text{Sr}$ of the exchangeable pool up to 320%.

Soil samples were collected over 715 days from the ^{84}Sr -treated area. To ensure $^{84}\text{Sr}/^{86}\text{Sr}$ values were representative for each of four sampling events and did not simply record heterogeneity of $^{84}\text{Sr}/^{86}\text{Sr}$ within the soil, we collected seven replicate soil cores during each sampling event (2.54 cm diameter) distributed randomly within seven subplots. Each core was separated into diagnostic soil horizons, and soil from replicate cores was combined to produce a single composite profile. Operationally defined plant-available cations were extracted from soils with 1 M ammonium acetate (NH_4Ac) and acid-digested as described above. The blank contribution of Sr^{2+} in the NH_4Ac extractant was <1 ppb, the detection limit of the atomic adsorption spectrophotometer used to measure Sr concentration.

Plant samples (*Drimys winteri*, family Winteraceae) were taken from 1- to 2-m tall saplings growing within and around the ^{84}Sr -labeled plot, as well as a fully mature 10-m tall individual (12.5 cm diameter at breast height) growing in the center of the plot. The drip line of this tree fell within the confines of the plot. Young leaves and buds were sampled, and xylem sap was extracted from shoots and cut branches by using a pressure

This paper was submitted directly (Track II) to the PNAS office.

Abbreviation: CPES, Cordillera Piuchué Ecosystem Study.

[†]To whom reprint requests should be addressed. E-mail: martink@mail.ucr.edu.

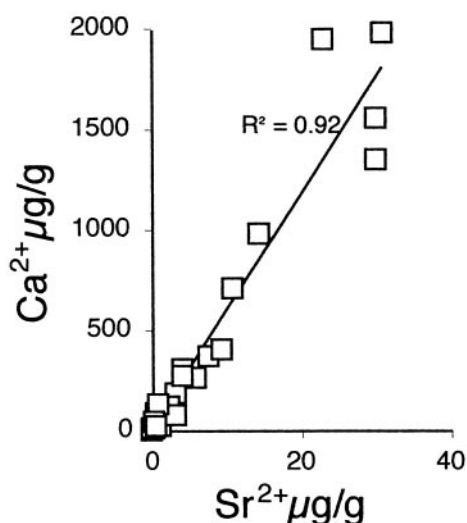


Fig. 1. Ca^{2+} $\mu\text{g/g}$ versus Sr^{2+} $\mu\text{g/g}$ of soil 1 m NH_4 acetate exchangeable soil solution showing a linear relation ($R^2 = 0.92$, $n = 24$) between Sr^{2+} and Ca^{2+} ions in solution, supporting the use of Sr^{2+} as a tracer of Ca^{2+} .

chamber. Plant samples were collected on three occasions over 404 days after spike addition and coinciding with soil sampling events. Application of the ^{84}Sr -labeled spike was timed to coincide with initial summer growth in the CPES forest to optimize the chance of ^{84}Sr uptake.

Sr^{2+} for all isotopic studies was separated by using Eichrom (Darien, IL) Sr-Specific Spec Resin in a class 1000 clean laboratory, and double-distilled acid was used for elution. Isotopic ratios were measured on a VG (Manchester, U.K.) Sector 54 with an external reproducibility of 0.00003 over 30 standard runs, and mass fractionation was normalized to $^{86}\text{Sr}/^{88}\text{Sr} = 0.1194$ by using an “exponential law” (20). Effects of the isotopically enriched tracer on the fractionation correction were adjusted off-line by using an iterative procedure. Base cations were measured on a Perkin–Elmer atomic absorption spectrophotometer (15).

Characterizing the $^{87}\text{Sr}/^{86}\text{Sr}$ of the Weathering and Atmospheric End-Members

The relative contribution of Sr^{2+} derived from atmospheric sources versus that originating from bedrock weathering can be determined if these sources have a distinct and readily characterized isotopic values that can be applied in a standard two-member mixing equation (4, 12–14, 18, 19). Determining these values is associated with uncertainties, however, because weathering and atmospheric inputs commonly derive from poorly characterized mixtures of sources rather than from single and temporally invariant sources. For example, atmospheric base cation inputs typically originate from several sources that can differ in $^{87}\text{Sr}/^{86}\text{Sr}$ signatures (e.g., crustal dust vs. marine aerosols) and can vary in strength over decadal periods (7, 8, 12). Weathering can be equally complex, involving combinations of different primary and secondary minerals, each with a particular (and poorly known) weathering rate and $^{87}\text{Sr}/^{86}\text{Sr}$ signature (12, 14). Further difficulties arise in cases where deposits of glacial or eolian materials introduce source materials that differ from bedrock $^{87}\text{Sr}/^{86}\text{Sr}$ values (4, 12, 14, 18, 21).

The predominance of marine aerosol greatly simplifies characterization of the atmospheric end-member at CPES, which can be taken as the $^{87}\text{Sr}/^{86}\text{Sr}$ ratio of seawater (0.70917) (16, 22). The weathering end-member is more problematic due to the heterogeneous mineralogy of the metasedimentary mica-shist bedrock, which contains quartz, biotite, muscovite chlorite, and

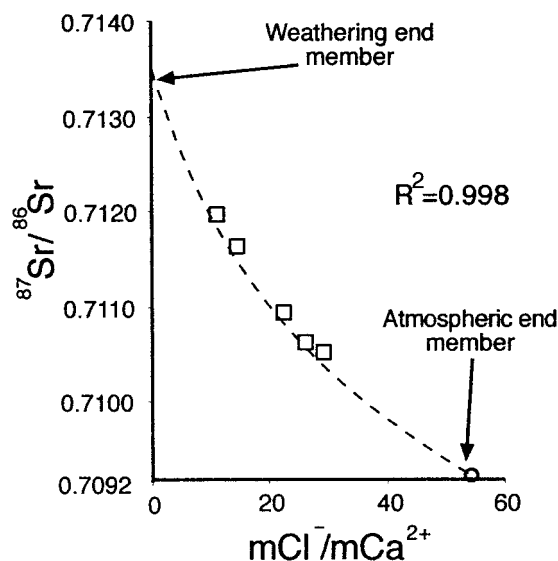


Fig. 2. Empirical relationship between $^{87}\text{Sr}/^{86}\text{Sr}$ and molar $\text{Cl}^-/\text{Ca}^{2+}$ ratios in CPES stream water (\square) and wet deposition (\circ). Measures over 3 yr demonstrated that the $\text{Cl}^-/\text{Ca}^{2+}$ weight ratio in wet deposition ($\bar{x} = 50$; $\text{SE} = 0.58$; $n = 62$) was within 6% of the ideal seawater molar ratio of ~ 56 (29). Samples collected throughout the year in which the weathering fraction (as determined by $\text{Cl}^-/\text{Ca}^{2+}$) ranged from 48% (high discharge) to 80% (low discharge). The curve is a mixing hyperbola fitted by a nonlinear least-squares (Levens–Marquadt) technique (30). The zero-chloride intercept is taken to represent zero precipitation input and the mean value of the isotopic ratio of Sr released to the catchment by weathering, providing a well-constrained weathering end-member ($^{87}\text{Sr}/^{86}\text{Sr} = 0.7134 \pm 1$). The Ca/Sr ratio of the weathering release is also well determined by the model ($\text{Ca}/\text{Sr}_{\text{wea}} = 251$). Data used within this plot are presented in Table 1.

Ca–Na feldspar (plagioclase) (15, 17). Because precipitation chemistry at the CPES site is almost exclusively derived from marine sources (15), we could constrain the $^{87}\text{Sr}/^{86}\text{Sr}$ weathering end-member based on coupling two independent tracer systems: $^{87}\text{Sr}/^{86}\text{Sr}$ and dissolved $\text{Cl}^-/\text{Ca}^{2+}$ ratios in soil and stream waters. Chloride is assumed a conservative tracer for sea-salt aerosol input (15), with the $\text{Cl}^-/\text{Ca}^{2+}$ of stream water modified by weathering addition of Ca^{2+} . At zero Cl^- concentration, all Ca^{2+} and Sr^{2+} should be weathering derived. We thus use the empirical relationship between $\text{Cl}^-/\text{Ca}^{2+}$ and $^{87}\text{Sr}/^{86}\text{Sr}$ in stream water and precipitation to estimate the mean $^{87}\text{Sr}/^{86}\text{Sr}$ ratio released by bedrock weathering in our study catchment (Fig. 2). An excellent fit to the stream water data is obtained with a nonlinear least-squares adjustment of a two-component mixing curve ($r^2 = 0.998$), and the $^{87}\text{Sr}/^{86}\text{Sr}$ weathering end-member can be taken as the zero-chloride intercept (0.7134) of the best-fit mixing hyperbola. The goodness of fit indicates that both the atmospheric and weathering sources have unique and well-defined end-members. The stream data provide a well-defined weathering end-member for $^{87}\text{Sr}/^{86}\text{Sr}$ and $\text{Ca}^{2+}/\text{Sr}^{2+}$, indepen-

Table 1. Stream water data

Sample collection	$^{87}\text{Sr}/^{86}\text{Sr}$	Ca, ppm	Cl, ppm
Stream water			
8/14/94	0.71094	0.16	3.14
2/8/95	0.71196	0.51	5.18
5/16/94	0.71063	0.18	4.20
11/11/95	0.71163	0.38	4.93
8/29/94	0.71052	0.15	3.97
Seawater	0.70917	411.00	19,400.00

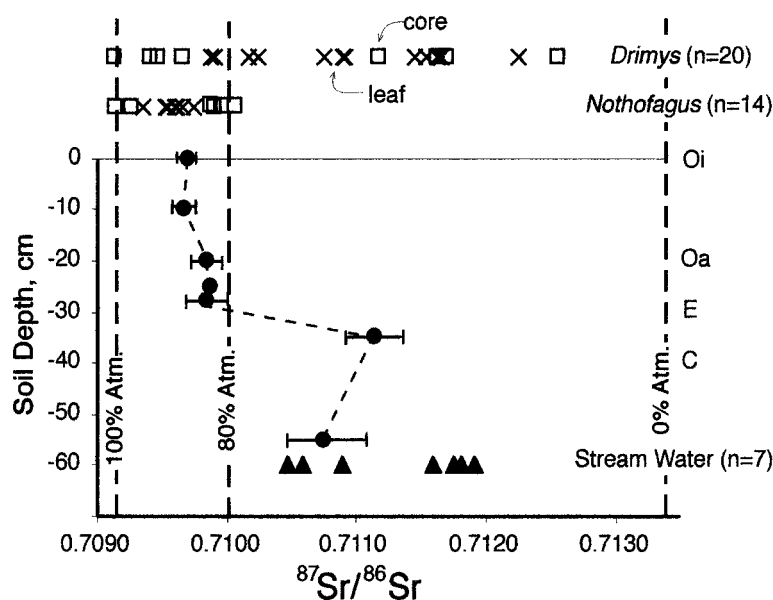


Fig. 3. Ratios of $^{87}\text{Sr}/^{86}\text{Sr}$ in different components of the CPES forest ecosystem. Changes in $^{87}\text{Sr}/^{86}\text{Sr}$ of the plant-available pool with soil depth (●) are averages from multiple samples collected from the same location over 2 yr ($n = 6$ for 0 cm depth; $n = 12$ for 20 cm; $n = 3$ for 25 cm; $n = 4$ for 28 cm; $n = 4$ for 35 cm; $n = 5$ for 55 cm). Error bars are the average of the distance from the mean for each depth (errors are smaller than the symbol at <25 cm depth). Stream water $^{87}\text{Sr}/^{86}\text{Sr}$ ratios (▲) are from seven independent events from two small watershed streams. Samples of plant material from *N. nitida* (12 individuals; $n = 14$) and *D. winteri* (eight individuals; $n = 20$) are identified by squares for core samples and crosses for leaf samples. Dashed lines identify the atmospheric marine aerosol end-member (0.70917), the weathering end-member, which was empirically derived in this study (0.7134), and 80% (0.7100) contribution from atmospheric sources. Percent atmospheric contribution was calculated by using a standard two-member isotope mixing equation (31).

$$\left(\frac{^{87}\text{Sr}}{^{86}\text{Sr}}\right)_{\text{sample}} = X_{\text{atm}} \times \left(\frac{^{87}\text{Sr}}{^{86}\text{Sr}}\right)_{\text{atm}} + (1 - X_{\text{atm}}) \times \left(\frac{^{87}\text{Sr}}{^{86}\text{Sr}}\right)_{\text{wea}}$$

where X_{atm} is the fraction of Sr^{2+} derived from the atmosphere, $(^{87}\text{Sr}/^{86}\text{Sr})_{\text{sample}}$ is the measured values of a sample, $(^{87}\text{Sr}/^{86}\text{Sr})_{\text{atm}}$ is the Sr isotopic composition of the atmosphere (marine values in this case or 0.70917), and $(^{87}\text{Sr}/^{86}\text{Sr})_{\text{wea}}$ is the Sr isotopic composition of the weathering end-member or 0.7134.

dent of any assumptions about weathering rates or the validity of leaching experiments (4) as an approximation of end-member weathering values.

Our empirical whole-watershed approach illustrates that the use of whole-rock (0.7360) or saprolite (0.7400) values would substantially overestimate the true $^{87}\text{Sr}/^{86}\text{Sr}$ weathering end-member in CPES soils, strongly biasing source attributions in favor of atmospheric inputs. This difference between whole rock ratio vs. actual weathering release can be explained by slower weathering (19, 23) rates of ^{87}Sr -enriched mica relative to ^{87}Sr -poor minerals such as plagioclase and chlorite in CPES soils.

$^{87}\text{Sr}/^{86}\text{Sr}$ Natural Abundance in Soils and Plants

Analyses of Sr isotopic abundances from different ecosystem components revealed that CPES forests depend primarily on cations of atmospheric origin. We show in Fig. 3 that $^{87}\text{Sr}/^{86}\text{Sr}$ ratios in the organic-rich shallow soil horizons reflect strong atmospheric contributions, with >85% atmospheric origin in the top 20 cm and >80% atmospheric origin in the top 30 cm of the soil profile. Weathering contributions increase abruptly in mineral horizons below 30 cm (37–46% weathering origin) and in stream waters (31–65% weathering origin).

Analyses of plant materials demonstrate that *Nothofagus nitida* (family Fagaceae), a dominant canopy species that constitutes >50% of total forest basal area (24), incorporates Sr^{2+} of atmospheric origin nearly exclusively ($\bar{x} = 91\%$ atmospheric source; SE = 1.7%; $n = 14$). We show in Fig. 3 that $^{87}\text{Sr}/^{86}\text{Sr}$ ratios vary little in *Nothofagus* (0.7091–0.7100) despite our efforts to change potentially important factors, including the size of trees (from 5 to 110 cm diameter at breast height) and location within the forest landscape. Eight similarly sized individuals (5

cm diameter at breast height) consistently display >87% contribution from atmospheric sources along a 700-m hill-slope transect, from upland moorland to near-stream forest habitats. In addition, $^{87}\text{Sr}/^{86}\text{Sr}$ ratios did not vary appreciably (range: 0.7099–0.7101) in three subsamples, each comprising 40 annual growth rings along a single *Nothofagus* tree core.

A second and less common tree species (*Drimys winteri*) displays a wider range in $^{87}\text{Sr}/^{86}\text{Sr}$ values (0.7091–0.7126) with five of eight individuals obtaining >89% of their Sr^{2+} from atmospheric sources (Fig. 3).

^{84}Sr Pulse Addition Results

Given the dominance of atmospherically derived base cations in the CPES system indicated by the $^{87}\text{Sr}/^{86}\text{Sr}$ data, we sought to determine the rate at which precipitation-delivered ^{84}Sr ions moves through the soil to be lost from the soil exchangeable pool by plant uptake or leaching losses. We show in Fig. 4 how $^{84}\text{Sr}/^{86}\text{Sr}$ in the plant-available pool changed with soil depth for up to 715 days after addition. Within Fig. 5A, we account for the mixing effects of the ^{84}Sr tracer within different-sized exchangeable Sr^{2+} pools in each successive soil horizon. The integrated value of ^{84}Sr across the soil profile (mass balance) (Fig. 5B) can be fit with a linear loss of the spike through time (zero-order kinetics), which predicts no remaining spike at 1,077 days after application. This high loss rate implies a soil turnover time of atmospherically derived cations of ≈ 3 yr. In contrast, turnover time calculated by using the entire ammonium acetate extractable Ca^{2+} or Sr^{2+} pools divided by the rate of total atmospheric deposition (wet + dry) gives an order of magnitude greater turnover time (29 yr for Ca^{2+} ; 27 yr for Sr^{2+}). This difference suggests either that the actual (functionally defined) Ca^{2+} pool

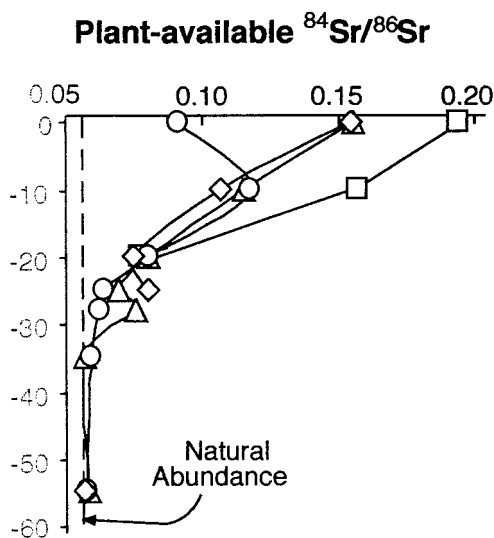


Fig. 4. Soil depth distributions of $^{84}\text{Sr}/^{86}\text{Sr}$ in plant-available pool at 0 days after (\square), 180 days after (\triangle), 404 days after (\diamond), and 715 days after (\circ) pulse addition of ^{84}Sr tracer to the soil surface. Individual data points are derived from a composite sample based on seven replicate soil profiles for each sample date. The dotted line signifies the fixed $^{84}\text{Sr}/^{86}\text{Sr}$ abundance in natural environments of 0.0565.

that turns over in the soil is substantially smaller than the pool determined by operationally defined extraction techniques and/or that internal cation cycles dominate the kinetics of Ca^{2+} and Sr^{2+} on soil exchange complexes. In either case, the results show that the dynamically available pool is small relative to fluxes of cations in and out of the soil, supporting the idea that soil pools of plant-available Ca^{2+} can be very sensitive to changes in atmospheric chemistry (e.g., changes in base cation or acid anion deposition) on time scales of decades (7, 8).

Concentration of ^{84}Sr closely parallels the depth distribution of plant-available Ca^{2+} and roots in the soil (Fig. 6), pointing to the role of shallow organic horizons in retaining cations within the soil-plant system. Despite the strong enrichment of ^{84}Sr within the root zone (Fig. 5A) and clear signs of added plant growth (buds and new leaves) after the tracer addition, the $^{84}\text{Sr}/^{86}\text{Sr}$ ratio did not rise above natural levels within *Drimys* samples ($n = 14$), indicating that the tree and saplings growing in the plot did not access the 1 m NH_4Ac extractable pool of Sr^{2+} we labeled with $^{84}\text{Sr}^{2+}$. This finding may largely reflect the deep root activity in *Drimys* implied by the wide range and more radiogenic values for natural $^{87}\text{Sr}/^{86}\text{Sr}$ for this species relative to *Nothofagus* (Fig. 3). The more radiogenic values suggest uptake from mineral horizons where $^{84}\text{Sr}/^{86}\text{Sr}$ values approach background levels. The complete absence of ^{84}Sr within plant parts is still surprising given the density of *Drimys* roots in the upper soil horizon, the abundance of readily available base cation nutrients in the upper organic-rich soil relative to the nutrient poor mineral soil (Fig. 6), and evidence of some strongly atmospherically influenced $^{87}\text{Sr}/^{86}\text{Sr}$ values within some *Drimys* leaves (Fig. 3). This finding may suggest the alternative possibility that plants are predominately fed by cations that are mineralized from soil organic matter rather than residing on exchange sites, thus creating two disconnected pools of cation cycling as indicated by the exceedingly rapid turnover of added ^{84}Sr .

Conclusions

Our results illustrate that although weathering is an important source of cations for stream water that exits CPES watersheds, shallow soil horizons and the dominant tree species are decoupled nutritionally from deeper weathering processes. With the exception of a few *Drimys* individuals, dominant trees nearly exclusively feed on Sr^{2+} and Ca^{2+} derived from shallow organic horizons, consistent with observed depth distributions of fine roots. The importance of shallow organic horizons can be further seen by the strong retention of ^{84}Sr tracer on cation exchange

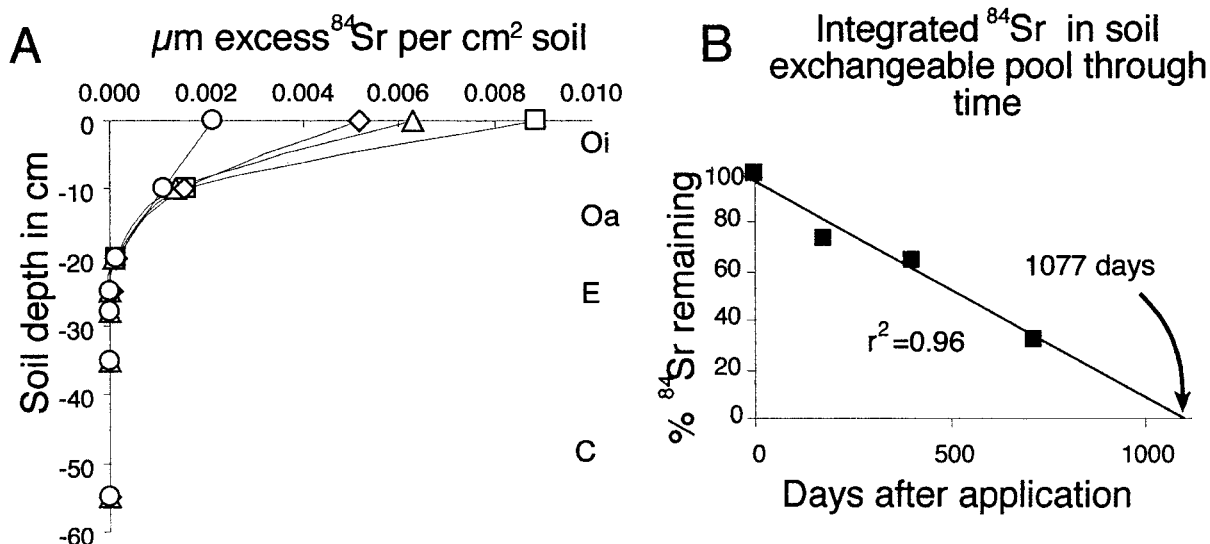


Fig. 5. (A) Excess ^{84}Sr within the exchangeable soil pool per soil horizon calculated by determining the amount of ^{84}Sr needed to alter the $^{84}\text{Sr}/^{86}\text{Sr}$ ratio to the measured value. An equivalent amount of ^{84}Sr added to a larger exchangeable pool will alter the $^{84}\text{Sr}/^{86}\text{Sr}$ less. The total pool is determined by integrating the measured concentration of exchangeable Sr^{2+} and the dry bulk density of the soil over the depth interval of a soil horizon. Depth and densities for the different horizons: Oi, (0–10 cm) 0.19 g/cm²; O, (10–20 cm) 0.19 g/cm²; Oa, (20–25 cm) 0.32 g/cm²; E₁, (25–28 cm) 0.32 g/cm²; E₂, (28–35 cm) 0.32 g/cm²; C₁, (35–55 cm) 0.4 g/cm²; C₂, (55–60 cm) 0.4 g/cm². Sr concentration and $^{84}\text{Sr}/^{86}\text{Sr}$ for each horizon are provided in Table 2. (B) Mass balance of ^{84}Sr over the 715 days of the study showing percent loss of initial ^{84}Sr addition (assuming all spike is recovered at time 0). Each point represents the total excess ^{84}Sr $\mu\text{m}/\text{cm}^2$ (from A and Table 2) summed for the seven soil horizons for a given sample interval. The integrated ^{84}Sr value shows a consistent linear decline less obvious in Fig. 4 because of the decline in exchangeable Sr^{2+} pool size with depth. The X intercept predicts from the linear regression identified, complete loss of ^{84}Sr after 1,077 days.

Table 2. Soil data from labeled plot

	Sr exchange, ppm*	Ca exchange, ppm*	⁸⁷ Sr/ ⁸⁶ Sr exchange [†]	⁸⁴ Sr/ ⁸⁶ Sr exchange [‡]	μmol/cm ² exch. ⁸⁴ Sr [§]	Recovery μmol ⁸⁴ Sr	% of 0 day
0 days							
Organic upper (0–10 cm)	30.8	1982.3	0.709981	0.19353	0.0044	0.0063	
Organic middle (10–15 cm)	7.5	370.3	0.709743	0.15730	0.0016		
Organic lower (15–25)	3.3	188.0	0.709707	0.07707	0.0002		100
180 days							
Organic upper	30.1	1349.6	0.709281	0.15530	0.0031		
Organic middle	10.9	708.4	0.709066	0.11589	0.0014		
Organic lower	4.1	305.1	0.709772	0.08023	0.0002	0.0047	
Eluted upper (26–30)	0.4	34.3	0.709794	0.06934	0.0000		
Eluted lower (31–40)	0.2	14.2	0.709527	0.07579	0.0000		76
C upper (41–50)	0.1	5.4	0.711165	0.05724	0.0000		
C lower (51–60)	0.1	6.9	0.711947	0.05884	0.0000		
404 days							
Organic upper	22.9	1941.0	0.709740	0.154870	0.0024		
Organic middle	14.6	978.0	0.709746	0.106671	0.0015		
Organic lower	6.0	259.0	0.709842	0.075197	0.0002	0.0042	
Eluted upper	2.5	124.0	0.709895	0.080520	0.0001		
Eluted lower	1.2	37.0	NA	NA	NA		66
C upper	1.3	27.0	NA	NA	NA		
C lower	0.6	86.0	0.710100	0.056739	0.0000		
715 days							
Organic upper	30.0	1550.6	0.709617	0.091359	0.0011		
Organic middle	9.3	405.7	0.709760	0.117641	0.0012		
Organic lower	4.3	269.4	0.710227	0.080225	0.0002	0.0026	
Eluted upper	3.1	71.6	0.709943	0.064279	0.0000		
Eluted lower	1.0	127.5	0.709528	0.062133	0.0000		40
C upper	0.3	38.2	0.711346	0.059610	0.0000		
C lower	0.6	20.6	0.711380	0.058146	0.0000		

NA, Not available.

*1 m NH4Ac exchangeable.

[†]⁸⁷Sr/⁸⁶Sr of the 1 M NH4Ac exchangeable soil fraction.

[‡]⁸⁴Sr/⁸⁶Sr of the 1 M NH4Ac exchangeable soil fraction.

[§]Integrated exchangeable ⁸⁴Sr within each horizon; see Fig. 5.

sites in upper soil horizons (Fig. 6). This view of CPES forest ecosystems points to the organic horizons as the key functional component that retains dilute atmospheric inputs of sea-salt cations and that allows recycling of these cations in forest ecosystem at turnover times of a few years, mechanisms that over

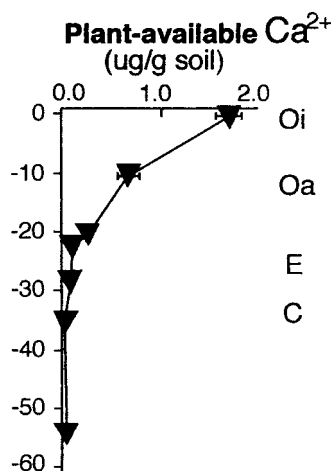


Fig. 6. Distribution of plant-exchangeable Ca²⁺ with soil depth from four sampling events during a 2-yr period. Horizontal bars show standard errors.

time permit the forest to become nutritionally decoupled from deeper weathering processes.

The close dependence of CPES trees on atmospheric sources challenges the prevalent paradigm that rock weathering is the dominant source of cation nutrition to plants (25, 26). While large annual precipitation volumes and unglaciated soils may enhance contributions of atmospheric sources relative to weathering in CPES forests, our results complement recent Sr isotopic studies of tropical ecosystems (18, 27, 28) that also indicate the important role of atmospherically derived nutrients. The broad range of ecosystems represented by these two studies support the general hypothesis (7, 27) that forest mineral nutrition can strongly depend on atmospherically deposited cations. The degree of vertical decoupling is most likely a function of several interacting factors: the soil depth at which dominant tree species “forage” for cations, the degree to which organic matter (with associated cation exchange sites and nutrients) accumulates in the soil, the frequency of disturbance events that cause deep mixing of the soil horizon (e.g., landslides) (28), and whether the forest grows on highly weathered geological substrates. For example, *Drimys* commonly grows as an early successional species colonizing areas of soil disturbance (most commonly landslides) in CPES forests. This finding suggests that its survival strategy includes deep feeding roots even in places where shallow, nutrient-rich soils may be present. Better understanding of how different tree species access nutrients spatially in soils might help explain why differences exist among species and/or

forests in sensitivity to acid rain and air pollution. For example, it is perhaps not surprising that forests dominated by shallowly rooted species, such as monocultures of Norway spruce (10), appear particularly sensitive to chronic cation loss.

We thank Juan Armesto, Cecilia Perez, Don José Nunque, and the Corporacion Nacional Forestal de Chile for site selection and field

logistic support; Juan Armesto, Michael Brown, Joseph von Fischer, Steven Perakis, Cecilia Perez, Don Jose Rios, Estrella el Cavallo, and Gail Steinhart for field and laboratory assistance; and Joel Blum, Tom Bullen, Art Johnson, and Dan Zarin for advice and comments on the manuscript. This work is a contribution to the Cordillera Piuchué Ecosystem Study and was supported by the A. W. Mellon Foundation and the National Science Foundation.

1. Falkengren-Grerup, U., Linnermark, N. & Tyler, G. (1987) *Chemosphere* **16**, 2239–2248.
2. Billett, M. F., Parker-Jervis, F., Fitzpatrick, E. A. & Cveassar, M. S. (1990) *J. Soil Sci.* **41**, 133–145.
3. Hallbäck, L. Z. (1992) *Pflanzenernähr. Bodenk.* **155**, 51–60.
4. Miller, E. K., Blum, J. D. & Friedland, A. J. (1993) *Nature (London)* **362**, 438–441.
5. Knoepp, J. D. & Swank, W. T. (1994) *Soil Sci. Soc. Am. J.* **58**, 325–331.
6. Likens, G. E., Driscoll, C. T. & Buso, D. C. (1996) *Science* **272**, 244–246.
7. Hedin, L. O. & Likens, G. E. (1996) *Sci. Am.* **275**, 88–92.
8. Hedin, L. O., Granat, L., Likens, G. E., Buishand, T. A., Galloway, J. N., Butler, T. J. & Rodhe, H. (1994) *Nature (London)* **367**, 351–354.
9. Johnson, A. H., Andersen, S. B. & Siccama, T. G. (1994) *Can. J. For. Res.* **24**, 39–45.
10. Schulze, E. D. (1989) *Science* **244**, 776–783.
11. McLaughlin, S. B., Tjoelker, M. G. & Roy, W. K. (1993) *Can. J. For. Res.* **23**, 380–386.
12. Graustein, W. C. & Armstrong, R. L. (1983) *Science* **219**, 289–292.
13. Åberg, G., Jacks, G. & Hamilton, P. J. (1989) *J. Hydrol.* **109**, 65–78.
14. Bailey, S. W., Hornbeck, J. W., Driscoll, C. T. & Gandette, H. E. (1996) *Water Resources Res.* **32**, 707–719.
15. Hedin, L. O., Armesto, J. J. & Johnson, A. H. (1995) *Ecology* **76**, 493–509.
16. Galloway, J. N., Keene, W. C. & Likens, G. E. (1996) *J. Geophys. Res.* **101**, 6883–6897.
17. McElroy, H. G. (1996) Master's thesis (Bryn Mawr College, Bryn Mawr, PA).
18. Kennedy, M. J., Chadwick, O. A., Vitousek, P. M., Derry, L. A. & Hendricks, D. M. (1998) *Geology* **26**, 1015–1018.
19. Capo, R. C., Stewart, B. W. & Chadwick, O. A. (1998) *Geoderma* **83**, 515–524.
20. Russell, W. A., Papanastassiou, D. A. & Tombrello, T. A. (1978) *Geochim. Cosmochim. Acta* **42**, 1075–1090.
21. Dahms, D. E., Shroba, R. R., Gosse, J. C., Hall, R. D., Sorenson, C. J., Reheis, M. C., Taylor, A. & Blum, J. D. (1997) *Geology* **25**, 381–382.
22. Dia, A. N., Cohen, A. S., O'Nions, R. K. & Shackleton, N. J. (1992) *Nature (London)* **356**, 786–788.
23. Blum, J. D. & Erel, E. (1997) *Geochim. Cosmochim. Acta* **61**, 3193–3204.
24. Armesto, J. J., Arayena, J. C., Perez, C., Smith-Ramirez, C., Cortes, M. & Hedin, L. (1994) in *Ecology of the Southern Conifers*, eds. Enright, N. J. & Hill, R. S. (Melbourne University Press, Melbourne, Australia), pp. 156–170.
25. Brady, N. C. (1994) *The Nature and Properties of Soils* (Macmillan, New York).
26. Schlesinger, W. H. (1997) *Biogeochemistry: An Analysis of Global Change* (Academic, San Diego), 2nd Ed.
27. Chadwick, O. A., Derry, L. A., Vitousek, P. A., Huebert, B. J. & Hedin, L. O. (1999) *Nature (London)* **397**, 491–497.
28. Vitousek, P. A., Kennedy, M. J., Derry, L. A. & Chadwick, O. E. (1999) *Oecologia* **121**, 255–259.
29. Berner, E. K. & Berner, R. A. (1996) *Global Environment: Water, Air, and Geochemical Cycles* (Prentice-Hall, Englewood Cliffs, NJ).
30. Bevington, P. R. & Robinson, D. K. (1972) *Data Reduction and Error Analysis in the Physical Sciences* (McGraw-Hill, New York), 2nd Ed.
31. Faure, G. (1991) *Principles and Applications of Inorganic Geochemistry* (Macmillan, New York).